Journal of Information Systems Engineering and Management
2025, 10(53s)
e-ISSN: 2468-4376
https://www.jisem-journal.com/

Research Article

Surface Finishing of Aluminum Alloys-3003 At Nano-Level Through use of Box-Behnken Experimental Design Methods by Magnetic Field-Assisted Finishing Processes

Sudhir Chaurasiya[1, a*] & Madhava Nand Pandey[1, b]
Adress[1]: Department of mechanical Engineering, National Institute of Technology, Patna, Bihar, Indian – 800005
Email: Sudhirc.ph21.me@nitp.ac.in[a] ,Email: mnpandey@nitp.ac.in[b]*

ARTICLE INFO

Received: 18 Dec 2024

Revised: 10 Feb 2025

Accepted: 28 Feb 2025

ABSTRACT:

This research investigates the application of the Magnetic field-assisted finishing process (MFAFP) by using a media of Magnetorheological fluid for nano-level surface finishing's ability to improve the practical and surface quality of materials is becoming more widely acknowledged. Surface roughness is reduced to the nanoscale by the MFAF process, which can enhance component performance. Traditional finishing methods cannot provide the necessary level of smoothness, which might cause problems with both performance and appearance. The novelty is that the nano-level surface finishing of aluminium alloy 3003 is by MFAF processes using the Box-Behnken Design (BBD) method. The process is designed to target a smooth surface at the nanoscale. The system parameter modifies the tool rotational speed, finishing time, and workpiece-tool gap to evaluate their impact on the surface finish. Initially, the surface roughness was found to be 380 nm. After the MFAF processes, its decrease of surface roughness to less than 15 nanometer was confirmed by measurements made using an optical profilometer and atomic force microscopy (AFM), and an even and flawless finish was revealed by using scanning electron microscopy (SEM) insights into surface morphology. The results demonstrated that the percentage change in surface roughness (%ΔRa) from (BBD) predicted responses was 93.37% value and from experimental value (%ΔRa) was found to be 96.0%, error found to be 2.74%, and the MFAF process significantly improved the surface quality of the aluminum alloy-3003. This study highlights that aluminium component performance and surface quality can be enhanced by using MFAF processes.

Keywords: Magnetic field assisted finishing (MFAF), Nano-Level Surface Finishing, Aluminium alloys 3003, Magnetorheological fluid (MRF), Box-Behnken Design (BBD).

INTRODUCTION

Magnetorheological (MR) fluid was slowly developed between the 1940s and the 1960s, making arrangements for wherever it would be applied [1]. Currently, it is used for a wide range of applications, such as the performance of mechanical dampers, clutches, break, isolation dampers, and refinements to surface finishes in several procedures. At the machining surface, up to the nano-level MR fluid is important, along with high-precision measurements of surface finish [2, 3]. As indicated by the wide variety of methods that have been tried and tested in this field, one of them is magnetorheological finishing. Stark disparities between conventional, nano-level processing and the use of MR fluid provide it with its unique edge in such processing areas. What separates it from other techniques is that it can achieve finishing nanometer-scale surfaces [4]. This is made possible by the determinate nature of the technology. Through changing the magnetic field strength of this process, careful regulation is made of the surface finish and the extensional strain resulting from it, forming two key factors under rheological control by which there will be no escape for maintaining surface integrity or promoting fatigue resistance in components [5, 6]. The MR fluid generally comprises magnetic particles a few microns in size suspended in a viscoelastic base medium. This non-Newtonian effect is due to the magnetic field intensity on MR-fluid, as well as moments as opposed to shear forces, which are the driving force necessary to begin successful activation. The type of base fluid- whether hydrocarbon-based or waterborne-casts- influences rheological properties and the feasibility of recycling, with formulations that

Journal of Information Systems Engineering and Management
2025, 10(53s)
e-ISSN: 2468-4376
https://www.jisem-journal.com/

Research Article

are waterborne often taking the edge in waste disposal, environmentally speaking [7]. In order to address the issues with the prepared MR fluid compositions, such as particle aggregation, which occurs primarily in water-based solutions as opposed to other base solutions, researchers created a new base medium called silicone gel base solution, added stabilizers like glycerol and grease oil to improve the overall performance of MR fluids during the finishing process [8]. In the sphere of MR finishing at the tooltip, the concentration of magnetic and abrasive particles, tool speed, and duration of machining are pivotal factors leading to surface quality. The interaction among these will eventually affect fluid flow properties and, by extension, efficiency in completion superfinishing [9].

However, much of that is above head--it matters, for example, what kind of abrasive powder or magnetic particle is employed and how strong these elements are in a solution. Research into MR finishing has covered a wide variety of materials and applications, starting from optical lenses to looks at typical metal parts and beyond [10]. Further, the technology transfer effect brought about by using MR finishing technology in future manufacturing ecosystems is a significant feature of this undertaking. There is also no need to be anxious about material wastage since MR finishing technology enables otherwise near-perfect control over such practices to hold that any other approaches (that is, which depart from its own) must seem wasteful energy-hungry by comparison. The author is in tune with the spirit of our times, and several movements aim to reduce the impact on the lab environment. This substance removal process of the MFAF process is studied. The method of MFAF processing is still not fully understood, and it is mainly a qualitative study. Constructing a multifield coupling theoretical model by combining electromagnetics, contact mechanics, elasticity, surface physical chemistry, and fluid dynamics is possible. Researchers will provide a comprehensive understanding of surface development and material removal in the MFAF process. The interaction between the media and the surface of a workpiece is researched using finite element simulation tools such as the Abaqus code. The removal of material using micro- and nano-abrasive media is also investigated. To gain a more in-depth comprehension of the material removal mechanism of MFAF, various pieces of analysis equipment, including a field-emission scanning electron microscope (FESEM), an X-ray photoelectron spectrometer (XPS), an atomic force microscope, and a comprehensive electrochemical analyzer, are utilized to investigate the micromechanical behaviour of the surface in micro and nanometer sizes. It includes friction, wear, surface contact stress distribution, and other similar phenomena [11]. The design and fabrications of the Magnetic Field Assisted Finishing tool from (Ansys Maxwell®) [12]. The Magnetic Field Assisted Finishing (MFAF) method polishes titanium alloy to a surface level of nanometres and gives you more control over the finishing forces [13]. Consequently, this method was selected as the last stage for polishing the bio-titanium alloy in the current investigation. The (MFAF) technique is one of the more contemporary methods that use the right polishing fluid composition to achieve ultrafine super finishing. This approach can cause minimal subsurface damage while producing an extremely high-quality surface finish. Abrasive particles are mixed with magnetorheological (MR) fluid to form the polishing medium in the MFAF process. Its elemental concentration and composition determine the rheological properties of MR fluid. The rheological qualities of the MR fluid are determined by its component concentration and makeup [14]. Stabilizers, abrasive particles, carbonyl iron particles (CIPs), and carrier fluids are all components of MR fluid [15].

Aluminum's high performance and economically advantageous properties—such as its low density, good castability, high working temperature, high resistance to corrosion, high strength, and high specific modulus—make it the most important and widely used material, even though many other materials are used in the aerospace, automotive, electronics, and construction industries to meet their needs [16]. More than 70% of the structural weight of a modern airplane is made of aluminum alloy, which is robust and resistant to damage. This alloy is utilized in the aircraft's most visible parts, such as the fuselage and wings. These properties are shared by aluminum alloys 7075 and 2024. Excellently finished aluminum alloys are frequently used in the fabrication of semiconductors, specialized telescopes, optical systems and sensors, microelectronic devices, and, to a considerable extent, wire conduction [17]. Aluminum mirrors with diamond cuts were manufactured to use as light collectors in a specialized telescope at Hanle, an Indian high-altitude observatory [18]. It is difficult to achieve good structural planarity and minimize surface scratches while chemically mechanically polishing aluminum because of its softness. Using traditional finishing techniques to achieve a nanoscale surface polish without sacrificing surface integrity is challenging because of aluminum's poor scratch resistance [19]. The micro/nano-machining (MNM) process is classified mainly into traditional and advanced. Most of the traditional MNM techniques are abrasive embedded; magnetic abrasive finishing (MAF) is one of the forms of MNM. Due to the fast rate of development in aerospace, electronics, optical, and nuclear industries, many

Journal of Information Systems Engineering and Management
2025, 10(53s)
e-ISSN: 2468-4376
https://www.jisem-journal.com/

Research Article

components of very complex geometry have required excellent surface finish and no surface defects, so ultra-precision machine finish is required [20, 21]. The traditional finishing process, polishing, and other finishing process cannot meet the demand of the new high-tech industry [22]. MAF works on both surface quality and the integrity of machine components. Among the MNM process, MAF plays an important role in nano finishing as it uses a magnetic field to force the magnetic abrasive particle into the workspace [23].

OBJECTIVES

The researcher investigates the superfinishing of aluminum alloy 3003 through magnetic-assisted finishing. The researcher employs the media of magnetorheological fluid (MR) and employs the analysis of variations (ANOVA) response methodology (RSM) of BBD models to optimize input parameters for investigating the effect of variations in the tool rotational speed process parameters, workpiece-tool gap, and surface finishing time on surface roughness. The experimentally observed value and the predicted value of the BBD model justify and also the optical profilometer, scanning electron microscopy (SEM) morphology, and atomic force microscope (AFM) topology picture of the surface of a workpiece, as well as the roughness (ΔRa).

METHODS

Material

Aluminum alloy 3003 is a commonly used alloy consisting primarily of aluminum with manganese as the principal alloying element. Because of its outstanding mix of strength, formability, and corrosion resistance, this aluminum alloy is among the most commercially available and adaptable. Commonly employed in applications needing strong corrosion resistance and lightweight, alloy 3003 is well-known for its manufacturing simplicity. Table 1 shows the chemical composition of Al-3003 alloys. The Energy dispersive X-ray spectroscopy chemical charecterization of Al-3003 alloys is illustred in Figure.1

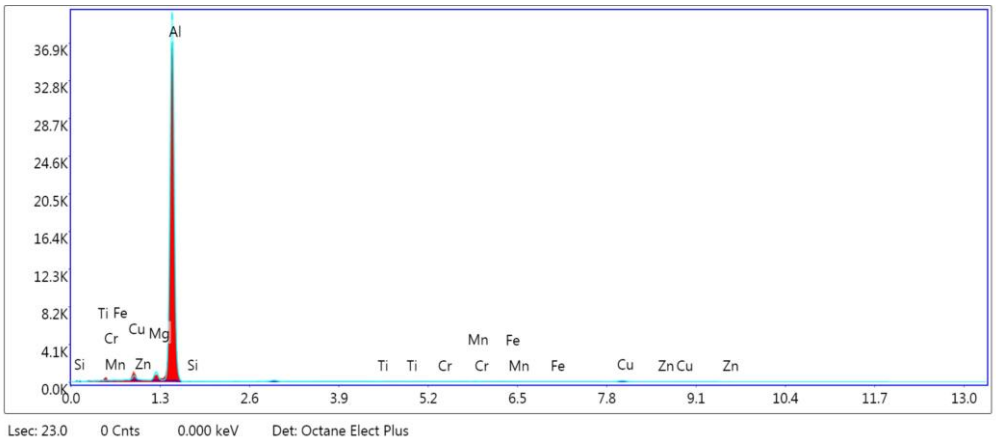

Figure.1: EXD spectroscopy elemental analysis of Al-3003-alloys

Table 1: Chemical Composition of Aluminum 3003

Material Alloy	Aluminium (Al)	Manganese (Mn)	Iron (Fe)	Silicon (Si)	Zinc (Zn)	Magnesium (Mg)	Copper (Cu)	Other elements
Wt.%	97%	1.2%	0.7%	0.6%	0.1%	0.05%	0.15%	balance

Magnetorheological Fluids (MR-fluids)

Journal of Information Systems Engineering and Management
2025, 10(53s)
e-ISSN: 2468-4376
https://www.jisem-journal.com/

Research Article

Magnetorheological fluids, often known as MRFs, are smart fluids that usually include a carrier fluid, such as oil, with the addition of magnetic particles. When exposed to a magnetic field, the fluid experiences a significant rise in its apparent viscosity, ultimately transforming into a viscoelastic solid [24]. The magnetorheological impact directly affects the mechanical properties of a fluid. It is a type of intelligent material that may alter its rheological and mechanical properties through contact with an external magnetic field. The MR fluid's suspended particles get magnetic and arrange themselves in a chain-like pattern according to the direction of the field. MR polishing fluids have several important properties, which are exhibits in Table 2. First and foremost is their high-yield stress under magnetic fields. Secondly, good dispersion is retained when compared to islands or instant fluids, which sink immediately on stopping the magnetic field but exhibit low off-state viscosity after removing magnetic fields. MR polishing fluids' excellent dispersibility makes producing a fine finish easier. In addition, unlike other low-viscosity organic solvent-based slurries, whether those containing several varieties of abrasive particles, MR permits quick recovery of fluids by centrifugal separation after use. He saves money so that the user can win an environmental award. Furthermore, the resilience to corrosion of MR polishing fluids is relatively high. For efficient polishing, perfect magnetic and abrasive particle concentrations must be attained. It yields fast finishing speeds and avoids agglomeration [24].

Table 2: Significances of MR fluid [24]

Constituent	Significance	Description
Magnetic Particles (CIPs)	Create the MR effect	Carbonyl iron particles (micron-sized)
Abrasive Particles	Responsible for finishing	Embedded non-magnetic particles in the fluid
Carrier Solvent (base fluid)	Rheological effects	Medium for suspending particles
Stabilizers	Minimize sedimentation of particles.	Agents for enhancing fluid stability and performance

MR Polishing Fluid Composition

The formulation of MR polishing fluids significantly impacts the surface quality of workpieces. Key parameters like homogeneity, apparent viscosity, and temperature are critical for managing material removal. The MR fluids typically contain micro-size magnetic carbonyl iron particles (CIPs), with non-magnetic abrasives suspended in carrier base fluids solvent and stabilizers. CIPs increase the MR fluid's strength when a magnetic field is introduced. At the same time, polishing abrasives increases the rate at which material is removed (MRR). The compositions of these fluids change depending on the materials that are being finished. Table 3 illustred compositions of sample volume is 1000 cm3, and the CIPs, SiC, and base fluid volumes have been set in specific volumes. In the MR fluid, the base fluid constitutes 60% by volume, while the remaining components comprise 20% SiC and 20% CIPs [25]. The volume of the prepared MR-polishing fluid is designated as 1.0 L, equivalent to 1000 cm^3. The CIPs are measured at 20 percent by volume, equating to 200 cm^3; weight amounts to 200 cm^3 multiplied by 7.8 gm/cm^3 (the density of CIPs), resulting in 1560 gm. Additionally, SiC abrasive constitutes 20 percent by volume, equating to 200 cm^3. Its weight is calculated as 200 cm^3 multiplied by 3.22 g/cm^3 (the density of silicon carbide abrasive powder), resulting in 644 g or 0.644 kg.

Table: 3. The Compositions of MR Polishing fluid [25].

Journal of Information Systems Engineering and Management
2025, 10(53s)
e-ISSN: 2468-4376
https://www.jisem-journal.com/

Research Article

Constituent	Concentrations %vol.	MR-fluids Compositions
Magnetic Particles	20%of vol.	Electrolytic Iron Powder
Abrasive Particle	20%of vol.	Silicon Carbide Powder
Base fluid (Carrier fluid)	60%of vol.	80% Heavy Paraffine oil
		20 grease Oil

The experimental Setup of MFAF process

The MFAF process experimental setup involves computer programming with a CPU connecting a 4-six CNC milling machine with a spindle attached to the rotation tool and fixed workpiece within a magnetorheological polishing (MRP) fluid solution to achieve the desired level of superfinishing of an external surface as shown in Figure.2 In this setup, The MR fluid is inserted concurrently between the magnetic tool and the workpiece fixed. A CNC milling machine rotates the magnetic tool, which creates a magnetic brush on the tooltip. This magnetic brush effectively removes material from the workpiece at the nano or micro scale, facilitating the attainment of a mirror-like polished surface in a comparatively shorter duration. The MR fluid is created by combining all of these components to conduct experiments, with a 4-axis CNC milling run through the given command from the CPU for a given input parameter.

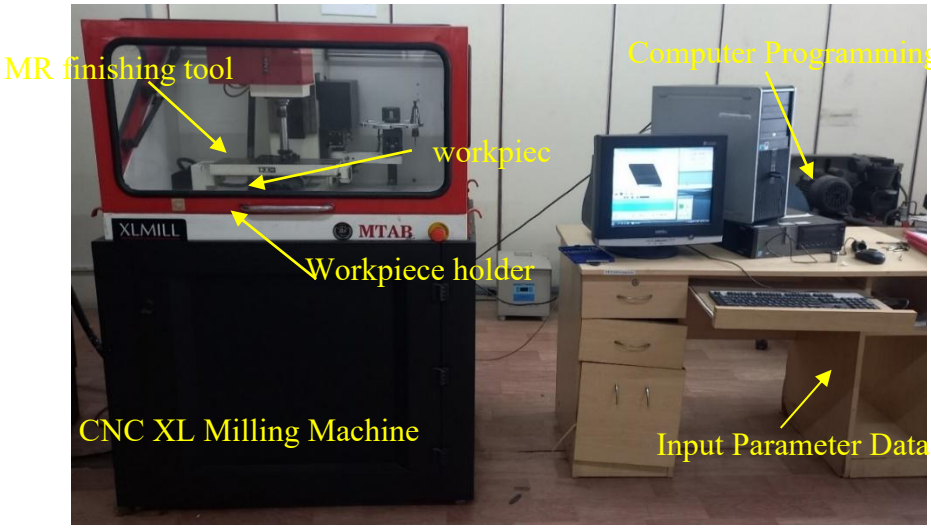

Figure.2: Schematical representations of MFAF process setup

Experimental Processes

The magnetic field-assisted finishing process, also known as MFAF-Processes, is a technique that shows great potential for producing super-finished freeform surfaces. The process involves utilizing a magnetic field to regulate the grinding power while employing magnetorheological fluid to aid the finishing procedure. The finishing action is carried out by it, which functions as a magnetic and lightweight abrasive brush. Additionally, a magnetorheological fluid is utilized to assist in the process. The MR fluids are spinning with the rotating tool, and the workpiece is fixed to achieve the intended result of relative motion between the finishing medium and the workpiece. With this apparatus, experiments were carried out to complete free-form assignments on aluminum alloy-3003. In this study, researchers are examining the effect of various parameters: the composition of MR fluid, the rotational tool, MR fluid properties, and time spent in finishes. The MR fluid acts as a sandwich between the tool and the surface of the workpiece. The tool finishing step introduces a given quantity of magnetic force through the MR fluid. On the one

Journal of Information Systems Engineering and Management
2025, 10(53s)
e-ISSN: 2468-4376
https://www.jisem-journal.com/

Research Article

hand, cutter media abrasive particles produce the combined tangential shear and regular magnetic forces that eliminate surface workpieces of many micro-afraid peaks and scratches, changing workpiece geometry to improve textures, surface morphology, and integrity.

Figure. 3(a) illustrated the fabrications of the MFAF tool and Figure. 3(b) is a representation of the computer-aided design (CAD) model that highlights the suggested MFAF tool configuration [12]. In this setup, the MR fluid takes on a spherical shape at the MFAF tool's tip due to the magnetic field, and abrasive particles are repelled toward the workpiece's surface, resulting in a superior surface finish. The force driving the finishing processes is the centrifugal force, operating through the shear mechanism.

In the experimental process, the researcher observed a slow and progressive degradation in the consistency of the MR fluid, illustrated by the steadily reduced viscosity and yield stress after each testing phase. As a result, the researcher found that MR fluid replacement was not just a choice but a necessity after each run. This step was crucial in maintaining the consistency and effectiveness of our experiments. To optimize magnetic field generation, the researcher maintained a 0.6 to 1.2 mm distance between components. The surface roughness was quantified by measuring workpiece dimensions before and after the finishing process. Overall, the research underscores the intricate interplay of parameters in MFAF and provides valuable insights for optimizing the finishing process to achieve superior surface quality.

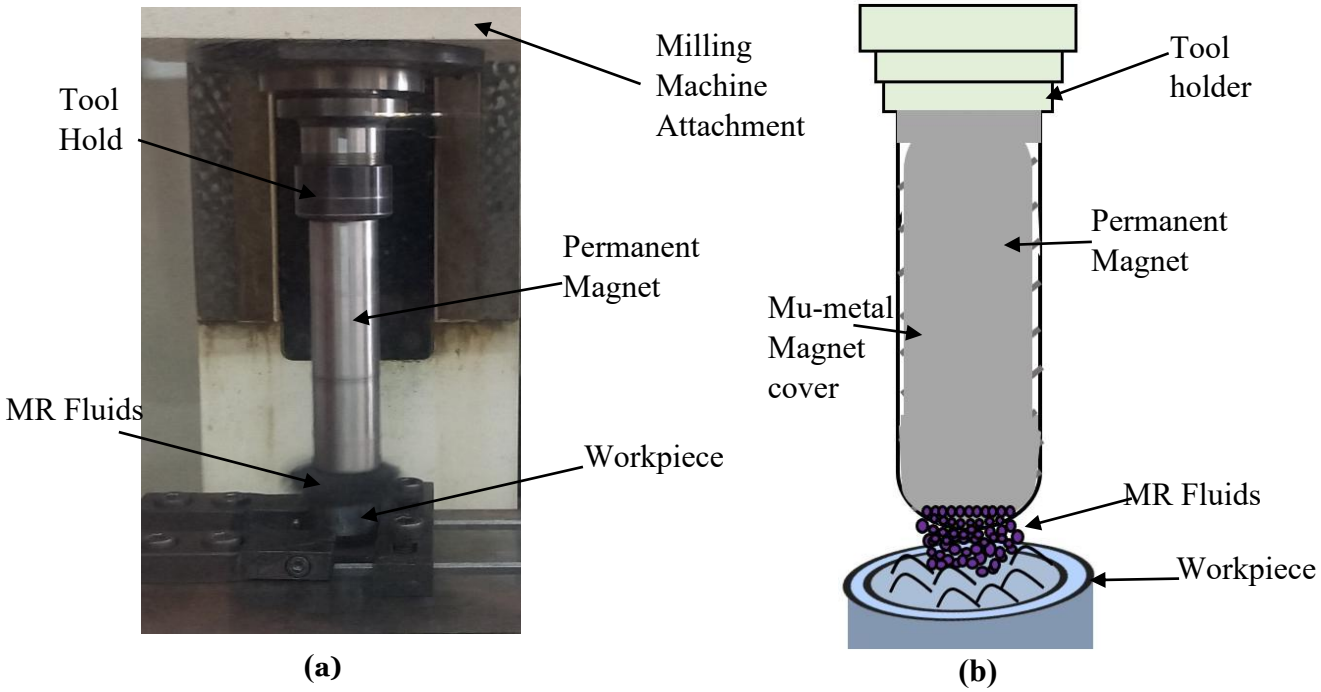

Figure. 3: Schematic of Experimental Setup for MFAF Process (a) Actually fabrications of MFAF tool (b) 3D design of CAD modal MFAF tool.

Analysis of magnetic field

In order to examine the magnetic flux generated by the permanent magnet at various sites, a magnetic field analysis is carried out. The rare-earth magnets based on neodymium, iron, and boron (NdFeB) with a 25 mm diameter and an 80 mm length have chosen to generate an external magnetic field in order to stiffen the MR fluid, which is then employed as a polishing medium. The compared to other permanent magnets on the market, NdFeB has superior magnetic characteristics and belongs to the rare-earth magnet family. And on the other hand, permanent magnets' magnetic fields are mostly determined by their dimensions and forms. The permanent magnets generate a magnetic field according to the formulas given by Maxwell (1)– (5).

Journal of Information Systems Engineering and Management
2025, 10(53s)
e-ISSN: 2468-4376
https://www.jisem-journal.com/

Research Article

$$\nabla . B = 0 \quad (1)$$

$$\nabla \, x \, B = -\frac{\partial B}{\partial t} \quad (2)$$

$$\nabla \times B + \frac{\partial B}{\partial t} = 0 \quad (3)$$

$$\nabla . D = \rho \quad (4)$$

$$\nabla \, x \;\; H = \hat{\jmath} + \frac{\partial D}{\partial t} \quad (5)$$

In the case of a closed surface, the total magnetic flux density is zero, as stated in (1). Furthermore, the net movement of current leaving the enclosed space, as given in Equation (2), equals to the ($-v_e$) rate of magnetic field in it. Based on Equation (3), the rate of change of magnetic field density forms plus the corresponding net electromotive force equal to zero. In addition to this, the total of the current density ($\hat{J}$) plus the displacement current equals the magnetomotive force acting on a closed surface on Equations (5). Seen from the following equation, the magnetic field (H) and its variations are mostly affected by the permeability of free space(μ_o) of the material and are proportional to the magnetic field density (B), as given Equations (6). As shown in the following equation. (7), H is calculated by the gradient of the magnetostatic scalar potential (Φm).

$$B = \mu_o H \quad (6)$$

$$H = -\nabla \, \Phi m \quad (7)$$

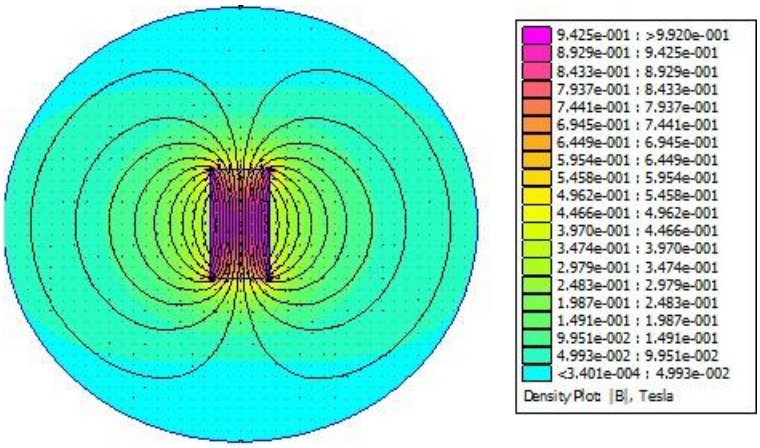

Figure.4: FEA study of magnetic field dispersion

Fig.4 The magnetic field distributions of the MFAF tool. At the center of the tool the magnetic field density is higher than at its end. In addition, the field density variations are 0.87 tesla at the center and 0.52 tesla at extremes for this equipment. A numerical method known as the finite element method (FEM) analysis for magnetic field distributions is used in the process of finding solutions to issues that are associated with electromagnetic fields. In the context of magnetic fields measure from Gauss meter, finite element method (FEM) enables the modelling of how magnetic fields behave in a variety of geometries, materials, and under a variety of boundary conditions.

Methodology and Design of Expert

Researchers employ experimental methods to learn about the impacts of different factors on nano-level surface finishing with magnetic field assisted finishing process (MFAFP) used by magnetorheological fluid (MRF). For this investigation, this study used the Box-Behnken Design (BBD) method from Response Surface Methodology (RSM)

Journal of Information Systems Engineering and Management
2025, 10(53s)
e-ISSN: 2468-4376
https://www.jisem-journal.com/

Research Article

[26]. A set of statistical and mathematical techniques sensitive to variables is known as response surface methodology. Both optimizing replies and discovering the variables' relationships to responses are possible using RSM. In these twenty experimental runs make up the BBD response surface design technique, which generates second-degree polynomial model variables. Although BBD considers all possible permutations of a variable's level, it shines when dealing with factors that include more than two variables. The BBD's strengths in analyzing experimental data, predicting model parameters, and aiding in the fitting of second-order polynomial models (which adequately represent the correlations between components and responses) make it an ideal tool for RSM. These are the reasons why BBD is utilized. Consequently, BBD is chosen for the purpose of creating trials for the input parameter tool rotational speed, working gap and, surface finishing time, effect of surface finishing investigations by MFAF process. The Equation (8) representing experimental runs are produced by the RSM-BBD using the second-degree polynomial model.

$$Y = \beta_0 + \sum_{i=1}^{k} \beta_i X_i + \sum_{i=1}^{k} \beta_{ii} X_i^{\,2} + \sum_{i=1}^{k-1} \sum_{j=i+1}^{k} \beta_{ij} X_i Y_j + e \qquad 8$$

In this context, Y is donated response variable of predicted, and independent variable are represented for X_i and Y_j level, and factor number is k, β_i is coefficient of linear for i^{th} factor, time of intercept is β_0, β_{ij} donated for coefficients of interaction in between i^{th} and j^{th} factor, and e is donated error.

The researcher uses Design Expert (version 11.1.2.0) to develop an experimental design setup in which the researcher performs trials with variables at three different levels and uses center points. Given the conditions, it is very likely that you are conducting an experiment using the Response Surface Methodology (RSM), a method often used to optimize processes or discover the ideal combination of components to maximize or minimize a response variable [27]. Use the Box-Behnken Design (BBD), the most typical approach for performing trials with three level of component design of input parameter as shown in Table.4. and the researcher used to the experimental design with response that is represented in the following Table. 5.

Table.4: Input factor parameter [28].

Factor	Name	Unites	Low Level	Center Level	High Level
A	Tool Rotational Speed	rpm	600.00	1200.00	1600.00
B	Working Gap	mm	0.6000	0.9	1.2
C	Finishing Time	hrs	4:30	6:30	8:30

The researcher measured surface roughness for all twenty experimental runs, with it mean values, for least three observations in each trial. The portable roughness tester KR210 measures initial and final surface roughness. In each MFAF procedure, every specimen's surface roughness was measured at multiple sites, and the average was analyzed. Table 5 shows the percentage change in surface roughness values from Equation 9.

$$\%\Delta Ra = \frac{\text{Initial value of (Ra)} - \text{final value of (Ra)}}{\text{Initial value of (Ra)}} \qquad 9$$

The Figure.5 illustreded the layout of working process during experimental and Anova analysis step by step upto validations of experimental results.

Journal of Information Systems Engineering and Management
2025, 10(53s)
e-ISSN: 2468-4376
https://www.jisem-journal.com/

Research Article

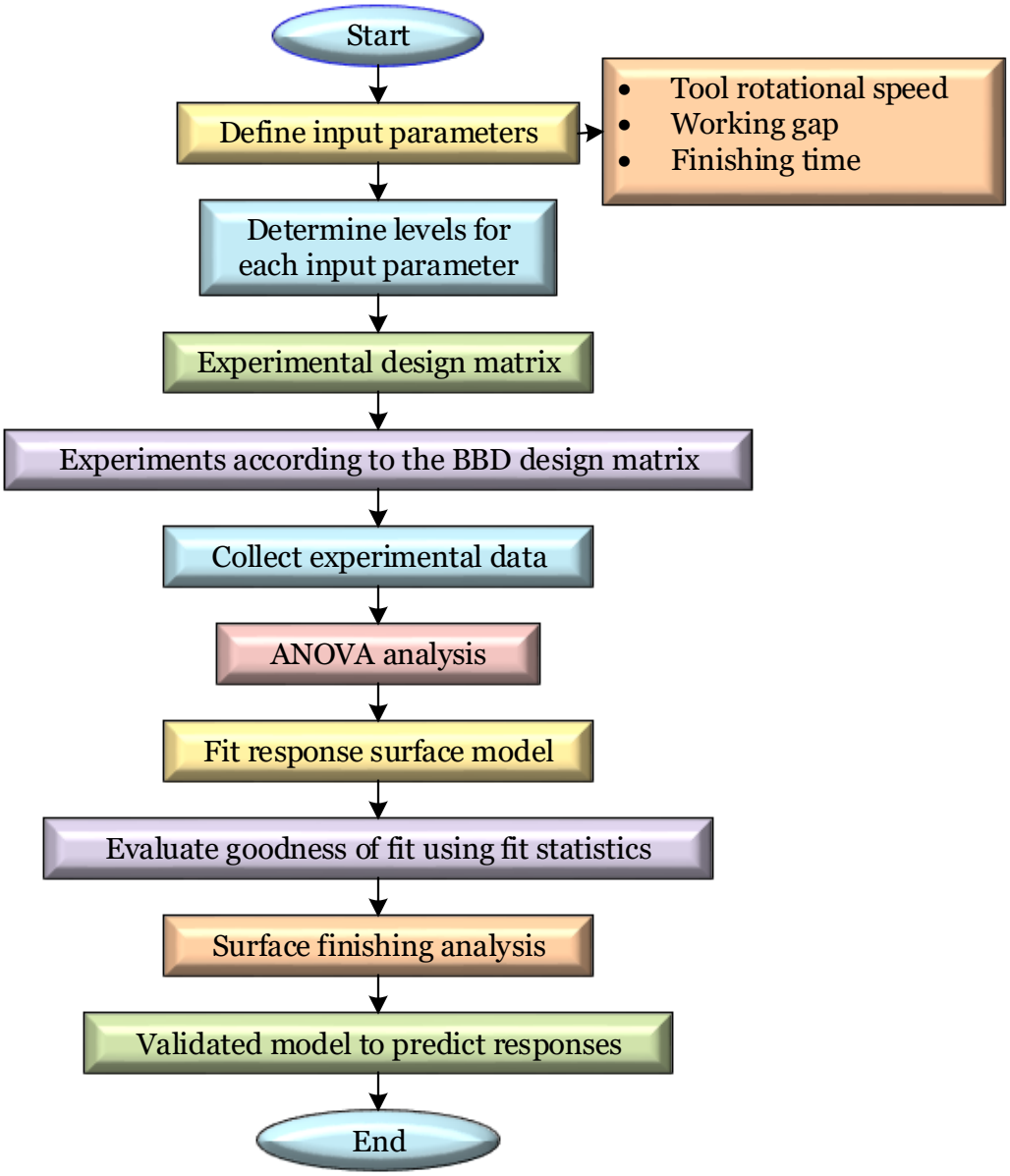

Figure.5: Steps in RSM-BBD

Table.5: Design of experiment with response summary

		Factor 1	**Factor 2**	**Factor 3**	**Response 1**
Std	Run	A:Tool Rotational Speed (rpm)	B:Working Gap (mm)	C:Finishing Time (hrs)	Percentage Change in Surface Roughness (%ΔRa)
1	1	600	0.6	6.3	67.35
18	2	1100	0.9	6.3	93.5
8	3	1600	0.9	8.3	79.15
2	4	1600	0.6	6.3	70.5

Journal of Information Systems Engineering and Management
2025, 10(53s)
e-ISSN: 2468-4376
https://www.jisem-journal.com/

Research Article

14	5	1100	0.9	6.3	93.12
12	6	1100	1.2	8.3	72
15	7	1100	0.9	6.3	93.75
13	8	1100	0.9	6.3	93.15
10	9	1100	1.2	4.3	77.12
16	10	1100	0.9	6.3	93.25
3	11	600	1.2	6.3	59
9	12	1100	0.6	4.3	70.5
5	13	600	0.9	4.3	66.75
20	14	1100	0.9	6.3	93.25
11	15	1100	0.6	8.3	89.6
17	16	1100	0.9	6.3	93.5
4	17	1600	1.2	6.3	67.15
19	18	1100	0.9	6.3	93.45
6	19	1600	0.9	4.3	60.85
7	20	600	0.9	8.3	62.5

RESULTS

Significance Statement The results presented in this work provide an understanding of the interlinked mechanics governing the surface characteristics obtained during the MFAF process by applying a Magnetorheological fluid (MRF). By scrutinizing the gathered data, researcher exposed the significant role played by each of the different parameters on the surface quality, including the rotational tool speed, workpiece material, finishing time, MR-fluid compositions and the working gap between the surface and the tool. Through our experimental analysis, researcher identified three critical process parameters to be utilized: rotational speed (in rpm), workpiece-tool gap, and surface finishing time. Due to the expected variation in the workpieces' surface roughness, the specified surface roughness (R_{ai}) as the primary independent variable. As researcher progressed with experiments, it observes a gradual decline in the consistency of MR fluid, with each source test phase showing lower viscosity and drop pressure than its predecessor.

Table.6: Results of the ANOVA for the quadratic model

Source	**Sum of Squares**	**df**	**Mean Square**	**F-value**	**p-value**	
Model	3385.00	9	376.11	8797.67	< 0.0001	significant
A-Tool Rotational Speed	60.78	1	60.78	1421.60	< 0.0001	
B-Working Gap	64.30	1	64.30	1504.00	< 0.0001	
C-Finishing Time	98.21	1	98.21	2297.25	< 0.0001	
AB	6.25	1	6.25	146.19	< 0.0001	
AC	127.13	1	127.13	2973.61	< 0.0001	
BC	146.65	1	146.65	3430.36	< 0.0001	
A^2	1595.49	1	1595.49	37320.21	< 0.0001	
B^2	345.17	1	345.17	8073.84	< 0.0001	
C^2	248.77	1	248.77	5818.99	< 0.0001	
Residual	0.4275	10	0.0428			
Lack of Fit	0.1032	3	0.0344	0.7427	0.5597	not significant

Journal of Information Systems Engineering and Management
2025, 10(53s)
e-ISSN: 2468-4376
https://www.jisem-journal.com/

Research Article

Pure Error	0.3243	7	0.0463			
Cor Total	3385.43	19				

From Table 6. the fact that the model has an F-value of 8797.67 is evidence that it is substantial and worthy of consideration. An F-value that is this large may be caused by noise, but the likelihood of this happening is very low—it's less than 0.06%. A p-value that is lower than 0.0500 indicates that the model terms are statistically significant. Within the context of this specific occurrence, the model terms A, B, C, BC, AC, AB, A^2, B^2 and C^2 are very important. Some values are more than 0.1000, which indicates that the model terms are not significant which means that they are not relevant. If your model has an occurrence that includes some inconsequential model terms (not counting those that are required to preserve hierarchy), the procedure of model reduction could prove to be advantageous for your model. There is not a significant difference between the pure error and the F-value for the lack of fit, which is 0.7427 according to the data. As a result of the existence of noise, there is a likelihood of 55.97% that a lack of fit F-value of this size may take place. Given that researcher want the model to be correct, it is preferable to have a lack of fit that is not very huge.

Table.7: Fit Statistics

	Percentage Change in Surface Roughness
Std. Dev.	0.2068
Mean	79.47
C.V. %	0.2602
R^2	0.9999
Adjusted R^2	0.9998
Predicted R^2	0.9994
Adeq Precision	234.0051
Lack of Fit (p-values)	0.5597

The Adjusted R^2 of 0.9998 is significantly different from the Predicted R^2 of 0.9994, which is greater than 0.2. This difference is more than what is typically expected. This may point to a serious issue with the data or models, or it may reveal a significant block effect. A few things to think about include outliers, model reduction, response transformation, and other similar issues. It is recommended to do confirmation run on all empirical models; it illustrates in Table.7.

One way to test the ratio of signal to noise is using Adeq Precision. Preferably, its ration needs to be more than 4. The ratio of signal to noise is 234.0051 is considered satisfactory. The design space may be explored using this model. Also, in the statics modal comparisons the press value is found to be 2.08, its illustred to Table.8.

Table.8: Statistics for modal comparisons

PRESS	2.08
-2 Log Likelihood	-20.15
BIC	9.80
AICc	24.29

Journal of Information Systems Engineering and Management
2025, 10(53s)
e-ISSN: 2468-4376
https://www.jisem-journal.com/

Research Article

Table.9: Coding Factors and Their Coefficients

Factor	Coefficient Estimate	df	Standard Error	95% CI Low	95% CI High	VIF
Intercept	93.37	1	0.0731	93.21	93.53	
A-Tool Rotational Speed	2.76	1	0.0731	2.59	2.92	1.0000
B-Working Gap	-2.83	1	0.0731	-3.00	-2.67	1.0000
C-Finishing Time	3.50	1	0.0731	3.34	3.67	1.0000
AB	1.25	1	0.1034	1.02	1.48	1.0000
AC	5.64	1	0.1034	5.41	5.87	1.0000
BC	-6.05	1	0.1034	-6.29	-5.82	1.0000
A^2	-18.68	1	0.0967	-18.90	-18.47	1.05
B^2	-8.69	1	0.0967	-8.90	-8.47	1.05
C^2	-7.38	1	0.0967	-7.59	-7.16	1.05

As shown in Table.9: taking into account the fact that all other factors remain same, the coefficient estimate shows the predicted response change per unit change in factor value. In a cross-sectional design, the intercept is the mean response over all runs. Factor settings determine the coefficients, which are modifications around that average. One indicates that the components are orthogonal, and a VIF more significant than one indicates multi-colinearity; a higher VIF indicates a stronger connection between the factors. In general, VIFs below 10 are considered reasonable.

Final Equations in turm of coded factor

To predict the outcome at any level of each element, one may plug the equation into the context of coded factors is shown Eqauation 10. In the default coding scheme, the factors at the levels are denoted by +1 for high and -1 for low. Comparing the coefficients of factors with the coded equation helps discover the relative effects of the elements.

$$\%\Delta R_a = 93.371250000000003411 + 2.75625000000000103029 * A + -2.834999999999997744 * B + 3.503749999999999698 * C + 1.2499999999999940048 * AB + 5.6374999999999984013 * AC + -6.0549999999999997158 * BC + -18.681875000000005116 * A^2 + -8.6893749999999982947 * B^2 + -7.3768750000000018474 * C^2 \quad 10$$

Final Equations in turm of actaull factor

Solving the equation regarding fundamental factors makes forecasting the reaction for specified levels of each component possible. Please provide the levels for each factor using their original units is shown in Equation11. However, this equation is useless for finding the relative effects of each component since the intercept is not in the precise centre of the design space, and the coefficients are changed to match the units of each element.

$$\%\Delta R_a = -166.94787968749955098 + 0.12689674999999936422 * \text{Tool Rotational Speed} + 218.74833333333194219 * \text{Working Gap} + 27.870281250000200401 * \text{Finishing Time} + 0.0083333333333334112802 * AB + 0.0056374999999999975478 * AC + -10.091666666666670338 * BC + -7.4727499999999741505e-05 * A^2 + -96.548611111110361094 * B^2 + -1.8442187500000151168 * C^2 \quad 11$$

Journal of Information Systems Engineering and Management
2025, 10(53s)
e-ISSN: 2468-4376
https://www.jisem-journal.com/

Research Article

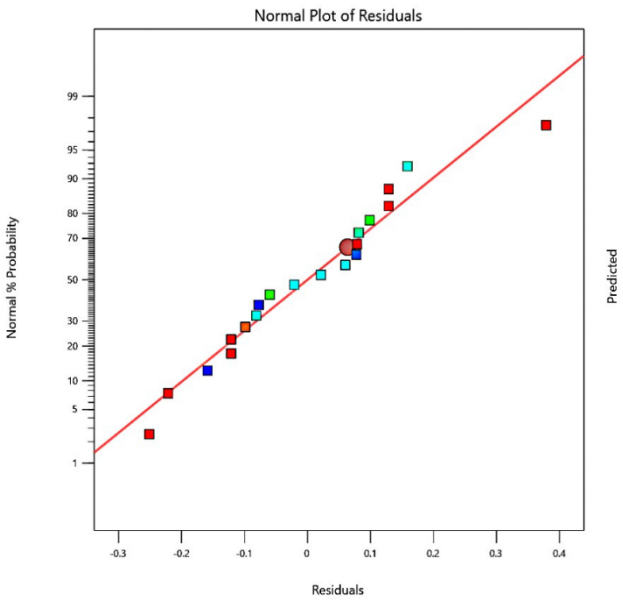

Figure.6: Normal Plot of Residuals

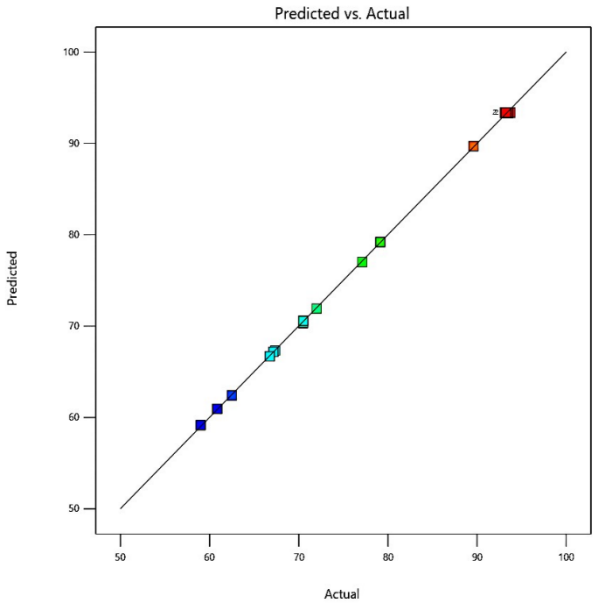

Figure.7: Predicted v/s Actual

As the compare the externally studentized residuals to the normal % probabilities and plot the graph according to Figure.6 One critical sign of the regression models' dependability is the close connection between these two components. Figure.7 shows the outcomes of the regression equations compared to the actual and anticipated responses; this, together with our other predictions, ensures that our R_a forecasts are robust.

In Figure. 8(a), the 3D plot illustrates the percentage change in surface roughness, which is represented along the Z-axis of the graph. In contrast, the working gap and rotational speed are plotted along the X and Y axes. As the rotational speed and working gap increase, the initial percentage change in surface roughness rises, reaching an optimum point before further decreasing. This information clearly explains how surface roughness fluctuates in a three-dimensional space. Most of the time, Figure. 8 (b) resembles a heatmap, utilizing colour coding to illustrate the changes in surface roughness. Red indicates a higher percentage change in surface roughness than yellow, while green represents the lowest change. The working gap and rotational speed influence the colour coding alongside the percentage variation in surface roughness. The robust analytical tool's response model can analyze the interrelationships among finishing time, working gap, percentage change in surface roughness, and their mutual effects, instilling confidence in the analytical approach.

To better appreciate the interactions between the change in surface roughness with changes in finishing time and tool rotational speed, Figure.9 (a) is a three-dimensional graphic that depicts the X-axis as the finishing time, the y-axis as the tool rotational speed, and the Z-axis as the change in surface roughness. Two-dimensional contour plots are shown in Figure.9 (b), highlighting the variations in surface roughness that occur when finishing time and tool rotational speed move independently. This example illustrates the variations in surface roughness via the use of colour. The shade of red has the most variation in surface roughness compared to the yellow and yellowish-green colours.

Figure.10 (a) shows the three-dimensional figure plotted along the Z-axis, representing the % change in surface roughness. Our approach relies heavily on this graphic, which shows the components that affect surface roughness holistically. For comparison, the 3D working gap is shown along the x-axis, and the completion time is shown along the y-axis. As the rational speed and working gap increase, the initial percentage change in surface roughness increases and reaching its optimum point further decreases; having this information provides a clear picture of how the surface roughness fluctuates in space that is three-dimensions, in most of the time the Figure.10 (b) resembles a heatmap and uses colour coding to show the change in surface roughness as red colour is showing the higher value

Journal of Information Systems Engineering and Management
2025, 10(53s)
e-ISSN: 2468-4376
https://www.jisem-journal.com/

Research Article

of percentage change in surface roughness as compared to yellow flow the green colour is lowest change in surface roughness. Colour coding is determined by the working gap and finishing time, with a % change in surface roughness as the determining factor.

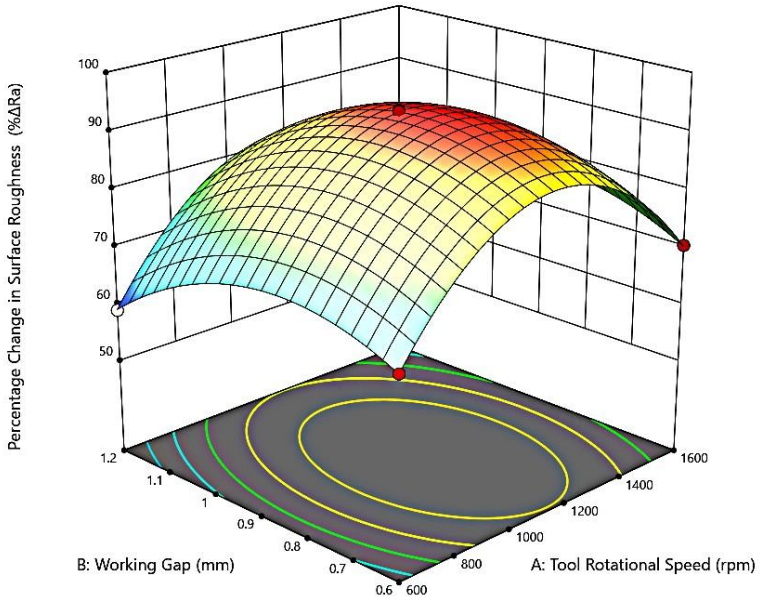

(a)

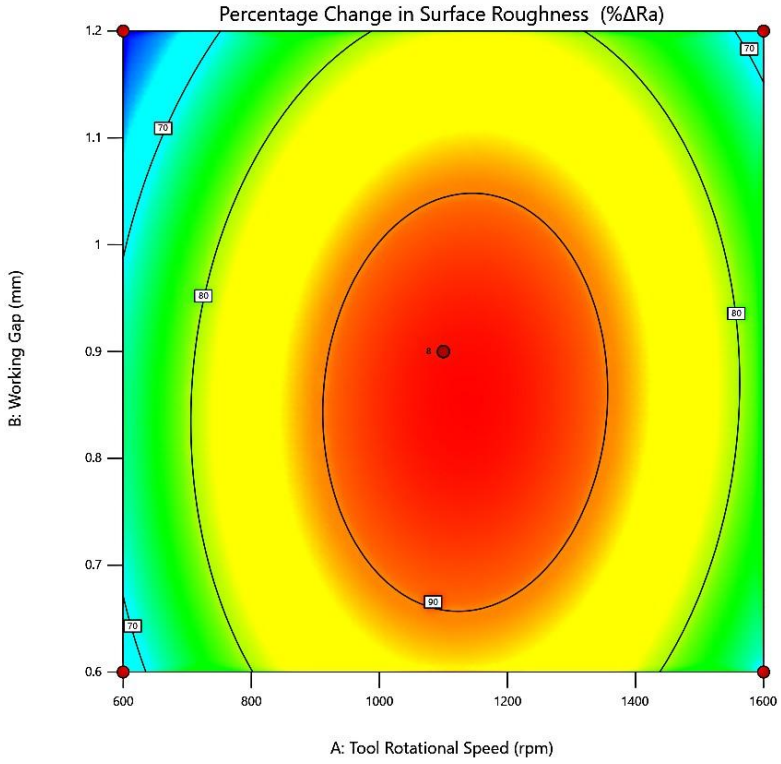

(b)

Figure.8: Percentages change in surface roughness (a) 3D Response surface plots (b) 2D Counter plots for rotational Speed vs working gap

Journal of Information Systems Engineering and Management
2025, 10(53s)
e-ISSN: 2468-4376
https://www.jisem-journal.com/

Research Article

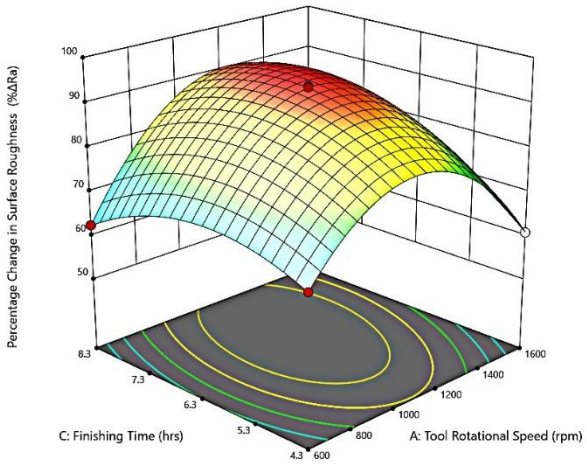

(a)

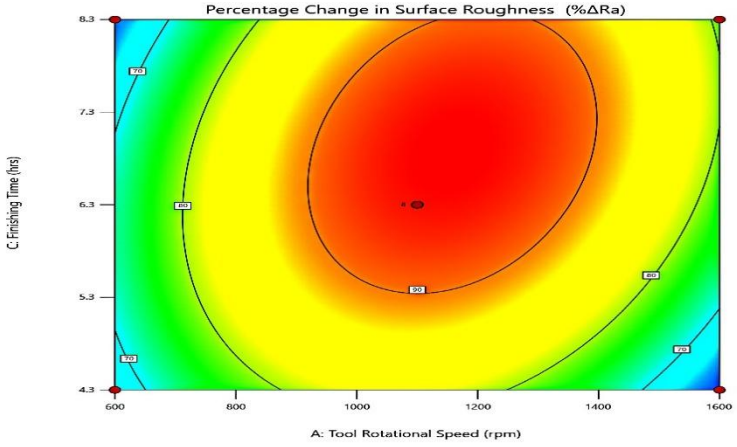

(b)

Figure.9: Percentages change in surface roughness (a) 3D Response surface plots (b) 2D Counter plots for rotational Speed vs finishing time.

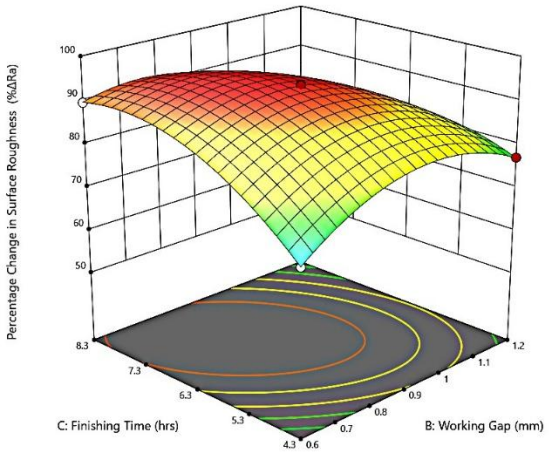

(a)

Journal of Information Systems Engineering and Management
2025, 10(53s)
e-ISSN: 2468-4376
https://www.jisem-journal.com/

Research Article

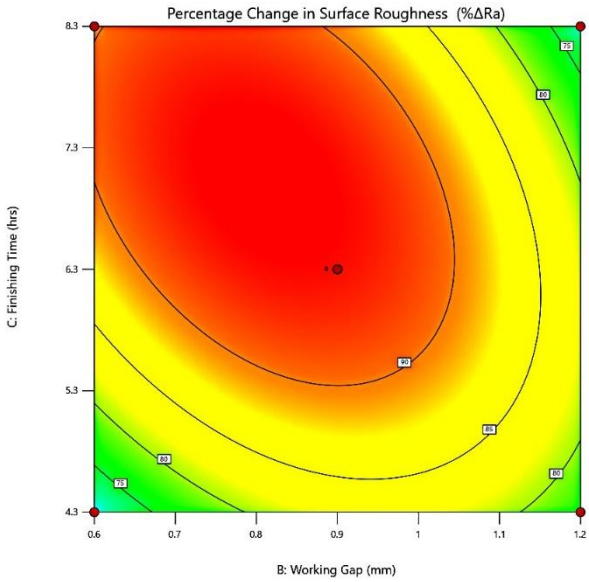

(b)

Figure.10: Percentages change in surface roughness (a) 3D response surface plots (b) 2D Counter plots for Finishing time vs working gap

DISCUSSION

From Anova response Table.2: total 20 experiments are runs; researcher identified three crucial parameters that played a significant role in the variability of surface roughness among workpieces. These parameters, namely tool rotational speed in revolutions per minute, workpiece-tool gap, and the time each face was finished, were instrumental in our research, with surface roughness (Ra) being our primary detached variable.

Effect on Surface finishing from tool rotation speed

The researcher's investigation into the relationship between tool speed and surface roughness reduction has practical implications for manufacturing and materials science. As the rotational speed of the tool increases, the %ΔRa also increases, indicating a reduction in surface roughness (Ra). This finishing procedure is optimized at a rotational speed of 1100 rpm. Further increases in tool speed led to a decrease in %ΔRa as the abrasive particles experience centrifugal force. The centrifugal force acting on the abrasive particles enhances their ability to wear down the surface of the workpiece, thereby improving the polishing effect. These findings can be applied to enhance the efficiency and quality of polishing processes in manufacturing.

The formula provided calculates the centrifugal force acting on abrasive particles. The force increases with the tool's speed, removing more abrasive material from the workpiece.

$$F_c = mr\omega^2 \tag{12}$$

Where $\omega = \frac{2\pi N}{60}$ and N is tool rotational speed in rpm

The polishing tool operates by utilizing a chain of abrasive particles and CIPs that form at the bottom of the tool. The centrifugal force grows as the tool speed increases, causing these chains to break and scatter outside the intended finishing zone. It is important to note that when the centrifugal force becomes too strong (above 1100 rpm), the CIPs chain breaks apart, and the dipolar magnetic force that holds the chains together is no longer sufficient, reducing the polishing efficiency. Figure. 11 visually demonstrates that beyond 1100 rpm, the increase in centrifugal force disrupts the abrasive chain formations, leading to a deterioration in surface finishing. Excessive tool speed can also induce

Journal of Information Systems Engineering and Management
2025, 10(53s)
e-ISSN: 2468-4376
https://www.jisem-journal.com/

Research Article

scratch marks on the workpiece surface, further deteriorating the surface roughness. This underlines the crucial role of the audience in maintaining the tool's operational limits and the need for caution when adjusting the tool's speed.

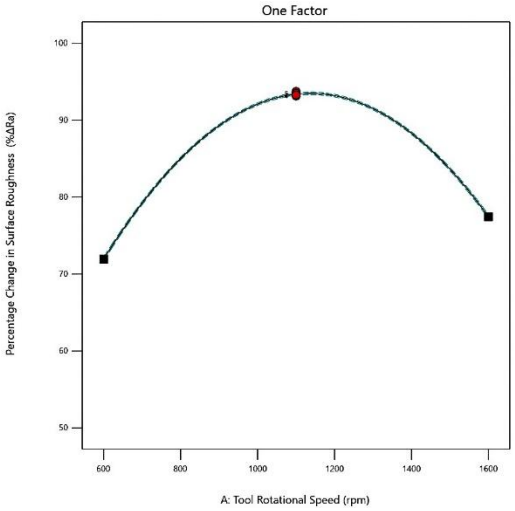

Figure.11: Effect on surface roughness from rotational speed

Effect on surface finishing from workpiece-tool gap

Through meticulous investigation, the researcher has uncovered the effect of working gaps on changes in surface roughness. At a small working gap (0.6), there is not enough space for a sufficient polishing medium to work effectively, which results in a poorer surface finish. However, as the working gap increases, the %ΔRa improves because the amount of polishing medium in the finishing zone increases, leading to more material removal. The polishing process involves CIPs and (colloidal abrasive particles) which are embedded in chains. With an increased working gap, the columnar structure of these chains becomes denser, and abrasive particles experience more force, enhancing the material removal process. The passage identifies an optimal working gap (0.9 mm) where %ΔRa peaks. Beyond this point, increasing the gap further reduces finishing effectiveness due to reduced magnetic flux density in the finishing zone. And becomes insufficient, reducing the finishing force on the abrasive particles leading to a decline in $\%\Delta R_a$.

Fig. 12 likely visually illustrates the changes in the CIPs chain structure as the working gap increases. With a smaller gap, there is a less pronounced columnar structure, whereas a more significant gap leads to a more developed and effective structure

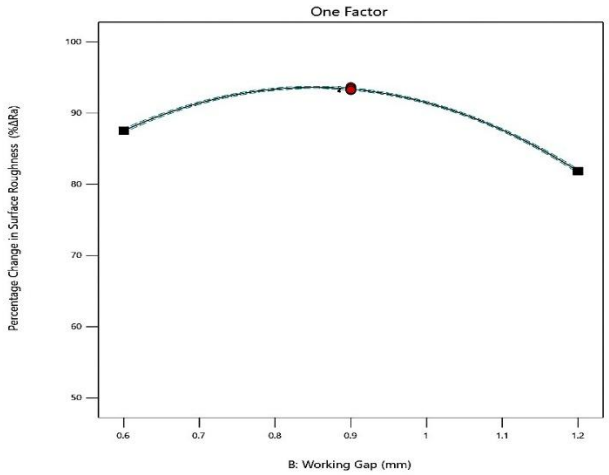

Figure.12: Effect on surface roughness from workpiece-tool gap

Journal of Information Systems Engineering and Management
2025, 10(53s)
e-ISSN: 2468-4376
https://www.jisem-journal.com/

Research Article

Effect of Surface finishing from finishing time

The researcher initially started the finishing process. The surface finishing time increased from 4:30 hrs to 8:30 hrs, and the change in surface roughness (%ΔRa) initially improves (increases), which means the surface gets smoother because of more time for the abrasive particles to work on the surface. However, after a certain optimal point (around 6:30 hrs), the %ΔRa increased again. This suggests that beyond the optimal finishing time, the abrasive is no longer improving the surface and instead starts to damage it by scratching the already polished

At 4:30 hrs, the surface shows deep scratch marks, indicating that the finishing is incomplete and the abrasive still aggressively interacts with the surface. After 4:30 hr, the scratches reduce, suggesting that the finishing process is progressing and the surface is getting smoother. At 6:30 hrs, the surface is well-finished with no visible scratches, showing the point of optimal surface quality. At 8:30 hrs, the scratches reappear, indicating that over-finishing damages the surface rather than improves it. The researcher highlights the importance of optimizing the finishing time to avoid diminishing returns. It suggests that there is a balance to be found- too little time leads to incomplete finishing, while too much time results in potential surface degradation. The key takeaway is that there is an optimal time range (6:30 hrs in this case) for achieving the best quality,

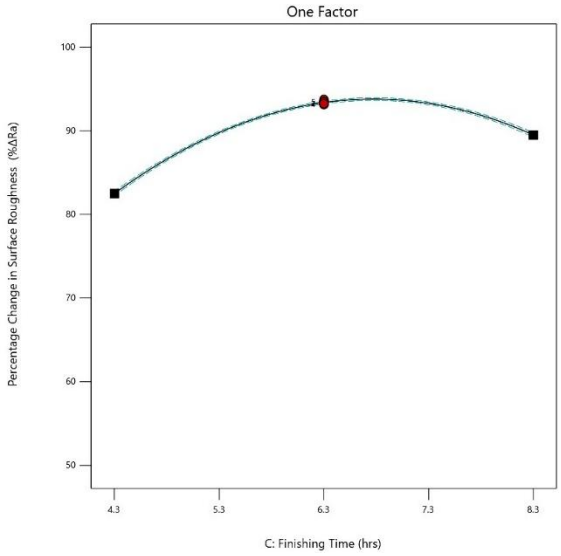

Figure.13: Effect of surface roughness from finishing time

Initially, the researcher measured the surface roughness Ra at 380 nm without polishing illustrated in Figure.14 from an optical profilometer. This surface roughness tester measures the surface smoothness without coming into contact with it. It offers non-destructive, high-resolution surface examination, which makes it particularly helpful for smooth or fragile surfaces that conventional contact-base profilometers might harm. Following the optimal MFAF process with a rotational speed of 1100 rpm, the workpiece-tool gap is 0.9 mm, and the finishing time is 6 hours 30 minutes. After completing the finishing process, the researcher measured the surface roughness of 15 nm. The researcher also justified the surface morphology image by scanning electronic microscopy (SEM) of the workpiece surface before and after the finishing process as shown in Figure.15, as well as from atomic force microscopy (AFM) topography images of the workpiece surface before and after the finishing process, as shown in Figure.16.

Journal of Information Systems Engineering and Management
2025, 10(53s)
e-ISSN: 2468-4376
https://www.jisem-journal.com/

Research Article

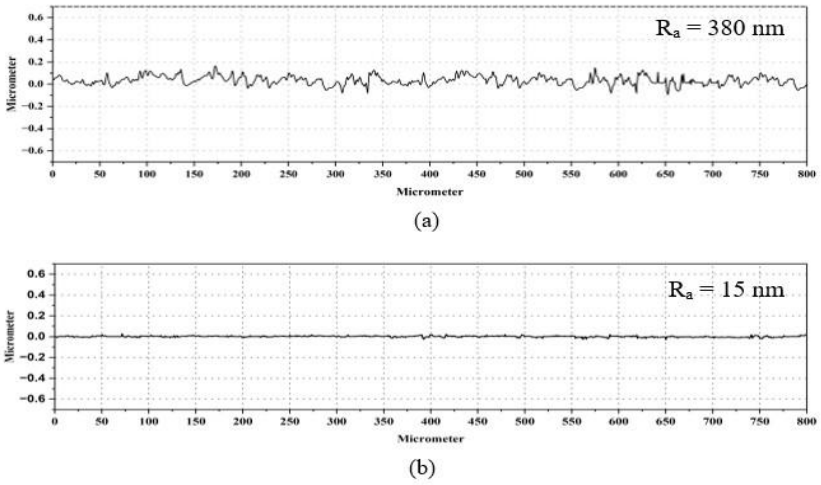

Figure.14: Surface roughness profile (a) Before MFAF process (a) After MFAF

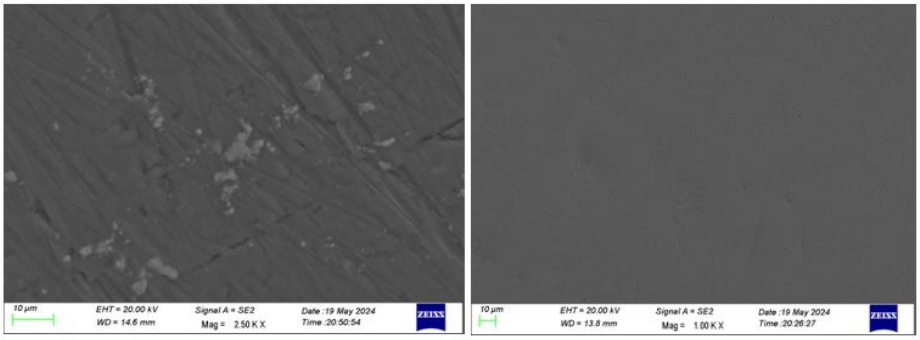

Figure.15: SEM surface morphology image of workpiece sample (a) Pre-Finishing (b) Post-Finishing.

Researcher are describing the result of the mirror finishing process on the Al-alloys workpiece. Based on your descriptions, the surface in Figure.17 (b) exhibits clear reflections of the text NITP on the finished surface, indicating that the surface has been polished to mirror-like after undergoing the MFAF (magnetic field assisted finishing) process. On the other hand, Figure.17 (a) shows the initial state of the workpiece surface, where no such reflections are visible, suggesting it was rougher and lacked the smoothness required for a mirror finish.

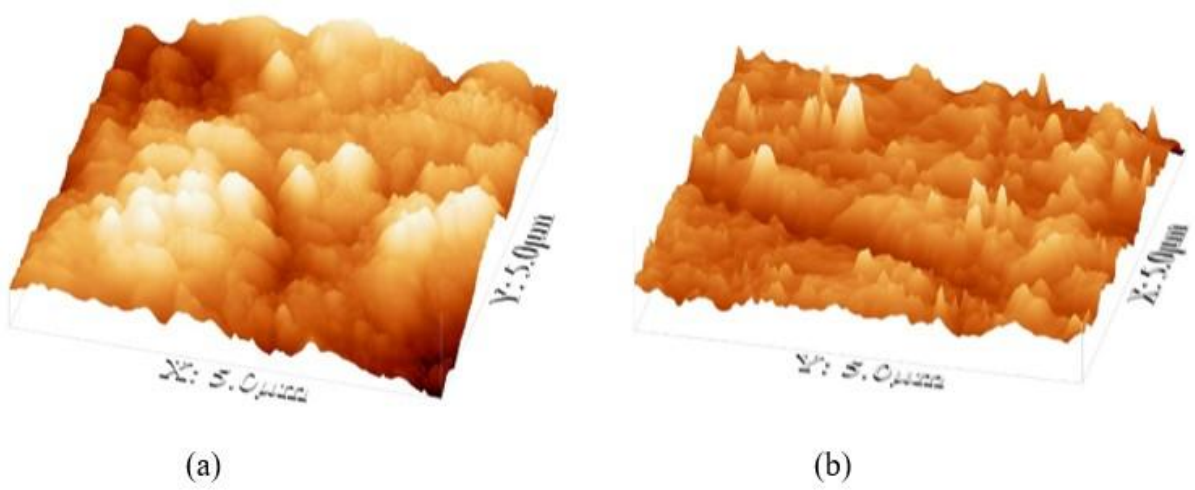

Figure.16: AFM surface topography image of workpiece (a) Pre-Finishing (b) Post-finishing.

Journal of Information Systems Engineering and Management
2025, 10(53s)
e-ISSN: 2468-4376
https://www.jisem-journal.com/

Research Article

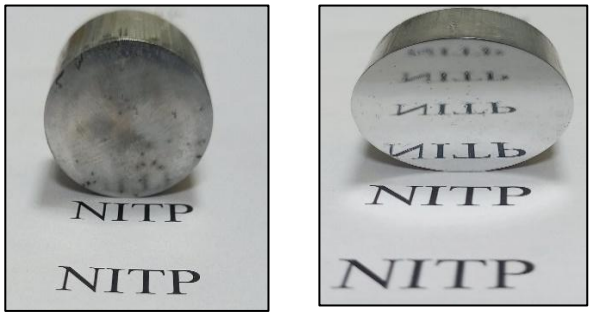

(a) (b)

Figure.17: Text image on workpiece surface (a) Before finishing (b) After finishing

Table.10: Confirmations Locations

Tool Rotational Speed (rpm)	Working Gap (mm)	Finishing Time (hrs)
1100	0.9	6.3

The analysis for response model confined confirmation location points, displayed in Table 10, could be utilized to conduct an experimental investigation at a pointed tool rotational speed of 1100 revolutions per minute, with a finishing time of 6:30 hours and a working gap of 0.9 millimeters. This investigation revealed an experimental result at confirmations location point for change in surface roughness of 96 percent, illustrated in Table.11.

Table.11: Result at confirm location point

Change in surface roughness (%ΔRa)	**Result**
	96.0%

Table.12: Point Prediction

Analysis	Predicted Mean	Predicted Median	Observed	Std Dev	SE Mean
Percentage Change in Surface Roughness	93.3713%	93.3713%	**96.0%**	0.206764	0.073102

The researcher found from the BBD response model to the point of prediction, as shown in Table 12, a powerful tool in analyzing BBD in RSM methodology, might be used to investigate the ways in which variations in completing time, working gap and % change in surface roughness predicted mean and predicted median are 93.3713%, which influence one another and the connections between variables.

Table.13: Validation of results

Analysis	Percentage Change in Surface roughness ($\%\Delta R_a$)	Error

Journal of Information Systems Engineering and Management
2025, 10(53s)
e-ISSN: 2468-4376
https://www.jisem-journal.com/

Research Article

Predicted value from BBD Response	**93.37%**	**2.74%**
Experimental result at confirmations locations	**96.00%**	

The validation of the result is shown in Table 13, where the predicted value of %ΔRa is 93.37%. This data comes from the analysis of variance (ANOVA) response of the BBD design model for the RSM technique. On the other hand, 96.0% is the percentage of %ΔRa, according to the tests carried out at the confirmatory sites, as shown in Table 11. The optimization results for %ΔRa changed by 2.74% of error from the experimental value.

CONCLUSION AND FUTURE PERSPECTIVES

This study has provided comprehensive insights into the parametric dependencies of the magnetorheological polishing fluids on MFAF process. Through various experiments, researcher observed that the surface finish, a critical outcome of this finishing technique, is influenced by factors such as rotational speed, the working gap, and finishing time. And also found that increasing the smoothness of the workpiece surface to 15 nm from an initial roughness value of 380 nm leads to a remarkable improvement in surface smoothness, a result that is sure to impress and intrigue. This comprehensive understanding of the process allows to predict the surface finish more effectively and empowers us to control it.

The researcher discusses the results from an experimental investigation, likely related to a machining or surface finishing process. In this context, the parameters mentioned (rotating at 1100 rpm, working with a 0.9 mm gap, and finishing at 6:30 hours) lead to the best surface finishing, which achieves a range of Ra 15 nm, which is quite impressive in precision machining. And it validates, the experiment's percentage change in surface roughness is a significant 96.0%, and the prediction response is 93.37% from the BBD method. The result of the error is found to be 2.74%,

In future research, the flow characteristics of Magnetorheological polishing fluid could be further analyzed. This includes studying its viscosity, flow parameters, and shear strength to understand the process dynamics better. Such investigations would contribute to refining the magnetorheological finishing technique and enhancing its efficiency and effectiveness in achieving superior surface finishes across various materials.

Data availability statement: All data that support the findings of this study are included within the article (and any supplementary files).

Declarations: The authors declare that they have no known competing financial interests or personal relationships that could have appeared to influence the work reported in this paper, and authors declare that there is no conflict of interest.

Ethics approval: This article contains no studies with human or animal subjects.
Consent for publication: NA.
Consent for participate: NA
Competing Interests: The authors declare that they have no competing interests**.**
Funding: No funding was received to carry out this research work

Sudhir Chaurasiya: https://orcid.org/0000-0002-0464-9785

REFRENCES

[1] C. Prakash, S. Singh, A. Pramanik, A. Basak, G. Królczyk, M. Bogdan-Chudy, Y. L. Wu and H. Y. Zheng, “Experimental investigation into nano-finishing of β-TNTZ alloy using magnetorheological fluid magnetic

abrasive finishing process for orthopedic applications," Journal of Materials Research and Technology, vol. 11, p. 600–617, 2021.
[2] M. Kumar, A. Kumar, H. N. S. Yadav, A. Alok and M. Das, "Abrasive based finishing method applied on biomedical implants: A review," Materials Today: Proceedings, vol. 47, p. 3985–3992, 2021.
[3] M. Kumar, H. N. Singh Yadav, A. Kumar and M. Das, "An overview of magnetorheological polishing fluid applied in nano-finishing of components," Journal of Micromanufacturing, vol. 5, p. 82–100, 2022.
[4] S. Kumar, V. K. Jain and A. Sidpara, "Nanofinishing of freeform surfaces (knee joint implant) by rotational-magnetorheological abrasive flow finishing (R-MRAFF) process," Precision engineering, vol. 42, p. 165–178, 2015.
[5] S. Kathiresan and B. Mohan, "Multi-objective optimization of magneto rheological abrasive flow nano finishing process on AISI stainless steel 316L," in Journal of Nano Research, 2020.
[6] P. Bhavsar and D. R. Unune, "Magnetorheological Polishing Tool for Nano-Finishing of Biomaterials," in Proceedings of the 10th International Conference on Precesion, Meso, Micro and Nano Engineering, 2017.
A. Barman and M. Das, "Generation of Nano-Level Surface Finish by Advanced Nano-Finishing Processes," Accuracy Enhancement Technologies for Micromachining Processes, p. 199–214, 2020.
[7] K. Sundararaj and M. Bangaru, "In Vitro Biocompatibility Study on Stainless Steel 316L After Nano Finishing," in ASME International Mechanical Engineering Congress and Exposition, 2017.
[8] F. A. A. Naji, Q. Murtaza and M. S. Niranjan, "Challenges and opportunities in nano finishing of titanium alloys for biomedical applications: A review," Precision Engineering, 2024.
[9] L. Nagdeve, V. K. Jain and J. Ramkumar, "Nanofinishing of freeform/sculptured surfaces: state-of-the-art," Manufacturing review, vol. 5, p. 6, 2018.
[10] Z. Yan, S. Yang, Y. Li, X. Li, W. Li and X. Yao, "Magnetic field-assisted finishing: mechanism, application, and outlook," The International Journal of Advanced Manufacturing Technology, vol. 131, p. 2719–2758, 2024.
A. Barman and M. Das, "Design and fabrication of a novel polishing tool for finishing freeform surfaces in magnetic field assisted finishing (MFAF) process," Precision Engineering, vol. 49, p. 61–68, 2017.
[11] S. Jha, V. K. Jain and R. Komanduri, "Effect of extrusion pressure and number of finishing cycles on surface roughness in magnetorheological abrasive flow finishing (MRAFF) process," The International Journal of Advanced Manufacturing Technology, vol. 33, p. 725–729, 2007.
[12] S. Jha and V. K. Jain, "Rheological characterization of magnetorheological polishing fluid for MRAFF," The International Journal of Advanced Manufacturing Technology, vol. 42, p. 656–668, 2009.
A. Sidpara and V. K. Jain, "Nano–level finishing of single crystal silicon blank using magnetorheological finishing process," Tribology International, vol. 47, p. 159–166, 2012.
[13] Sharma and M. S. Niranjan, "Chemical assisted ball end magnetorheological finishing of aluminium 7075 alloy," Ain Shams Engineering Journal, vol. 15, p. 102397, 2024.
[14] M. Peters and C. Leyens, "Aerospace and space materials," Mater. Sci. Eng, vol. 3, p. 1–11, 2009.
[15] R. RKoul, A. AMitra, A. C. H. A. R. Y. A. BS and T. VChitnis, "An update on the design and implementation of the MACE gamma-ray telescope," in International Cosmic Ray Conference, 2011.
[16] S.-Y. Chiu, Y.-L. Wang, C.-P. Liu, J.-K. Lan, C. Ay, M.-S. Feng, M.-S. Tsai and B.-T. Dai, "The application of electrochemical metrologies for investigating chemical mechanical polishing of Al with a Ti barrier layer," Materials chemistry and physics, vol. 82, p. 444–451, 2003.
[17] V. K. Jain, "Magnetic field assisted abrasive based micro-/nano-finishing," Journal of Materials Processing Technology, vol. 209, p. 6022–6038, 2009.
[18] G. Ghosh, A. Sidpara and P. P. Bandyopadhyay, "Review of several precision finishing processes for optics manufacturing," Journal of Micromanufacturing, vol. 1, p. 170–188, 2018.
[19] V. K. Jain, Nanofinishing science and technology: basic and advanced finishing and polishing processes, CRC Press, 2016.
[20] F. Mazzucato, "Development of a suitable modelling approach for the robot assisted polishing process".
A. Sidpara, "Magnetorheological finishing: a perfect solution to nanofinishing requirements," Optical Engineering, vol. 53, p. 092002–092002, 2014.
[21] D. A. Khan and S. Jha, "Selection of optimum polishing fluid composition for ball end magnetorheological finishing (BEMRF) of copper," The International Journal of Advanced Manufacturing Technology, vol. 100, p. 1093–1103, 2019.

Journal of Information Systems Engineering and Management
2025, 10(53s)
e-ISSN: 2468-4376
https://www.jisem-journal.com/

Research Article

[22] G. Chawla, R. S. Sharma and V. K. Mittal, "Box-Behnken Design for MAFM Precision Surface Finishing of Al-6063/SiC/B 4 C Composites: A Comparative Study with Nature-Inspired Algorithms," Fine Chemical Engineering, p. 1–30, 2025.
[23] S. Prakash, K. Palanikumar, J. Lilly Mercy and S. Nithyalakshmi, "Evaluation of surface roughness parameters (Ra, Rz) in drilling of MDF composite panel using Box-Behnken experimental design (BBD)," Int. J. Des. Manuf. Technol, vol. 5, p. 52–62, 2011.
A. Barman and M. Das, "Toolpath generation and finishing of bio-titanium alloy using novel polishing tool in MFAF process," The International Journal of Advanced Manufacturing Technology, vol. 100, p. 1123–1135, 2019.